Title

Microwave dielectric properties of tunable capacitors employing bismuth zinc niobate thin films

Journal

Journal of Applied Physics, 97

Authors

Park, Jaehoon
Lu, Jiwei
Stemmer, Susanne
et al.

Publication Date

2005

Peer reviewed

Microwave dielectric properties of tunable capacitors employing bismuth zinc niobate thin films

Jaehoon Park

Department of Electrical and Computer Engineering, University of California, Santa Barbara, CA 93106-9560

Jiwei Lu and Susanne Stemmer[a)]

Materials Department, University of California, Santa Barbara, CA 93106-5050

Robert A. York[b)]

Department of Electrical and Computer Engineering, University of California, Santa Barbara, CA 93106-9560

[a)] electronic mail: stemmer@mrl.ucsb.edu

[b)] electronic mail: rayork@ece.ucsb.edu

Abstract

Planar capacitors employing $Bi_{1.5}Zn_{1.0}Nb_{1.5}O_7$ (BZN) thin films with the pyrochlore structure were fabricated on platinized sapphire substrates. The total device quality factor and capacitance were analyzed in the microwave frequency range (up to 20 GHz) by measuring reflection coefficients with a vector network analyzer. The parasitics due to the probe pads were extracted from the measurements. The total device quality factor, which included losses from the dielectric and the electrodes, was more than 200 up to 20 GHz for devices with an area of 100 μm^2. Based on the frequency-dependence of the impedance, series losses of unknown origin appear to dominate the device quality factor at higher frequencies. No significant dispersion in the device capacitance, as would be associated with a dielectric relaxation of BZN, was measured. The large electric field tunability of the permittivity of BZN films and the high device quality factors make these films attractive for voltage controlled microwave devices.

I. INTRODUCTION

Thin films exhibiting an electric-field tunable dielectric constant are being investigated for microwave frequency agile devices, such as phase shifters and filters. In addition to a large tunability, these devices require dielectrics with low dielectric losses (tan δ). For room temperature applications, thin films of ferroelectrics such as $(Ba,Sr)TiO_3$ (BST) have been extensively studied [1]. Recently, thin films of a non-ferroelectric material, $Bi_{1.5}Zn_{1.0}Nb_{1.5}O_7$ (BZN), which has the cubic pyrochlore structure [2] and a medium permittivity (170 – 200), have attracted interest for tunable applications due to their very low losses (~ 5×10^{-4} [3]) and large tunabilities (55 %) [3-6] at low frequencies (~ 1 MHz). The tunability is defined as $(\varepsilon_{max} - \varepsilon_{min})/\varepsilon_{max}$, where ε_{min} is the minimum measured permittivity at the maximum applied field, and ε_{max} is the dielectric constant at zero bias.

BZN ceramics exhibit a low temperature dielectric relaxation, i.e., a time lag between the applied electric field and the polarization, that is accompanied by a dielectric loss peak [7,8]. This loss peak shifts to higher temperatures with higher frequencies, approaching room temperature in the microwave frequency region [7-9]. Therefore bulk BZN is believed to be not suitable for applications requiring low losses in the GHz frequency regime. However, thin films may have different properties. For example, we have recently shown that tensile film stresses, due to the thermal mismatch with a substrate, reduce the activation energy of the dielectric relaxation and require higher frequencies to shift the dielectric relaxation to higher temperatures [10]. Thus, BZN films may remain attractive for low loss, high frequency applications. To date, only one study has reported microwave dielectric measurements of BZN films at a single

frequency [11]. In this letter we report the dielectric response of BZN thin film capacitors over a broad frequency range in the GHz region. We show that very high device quality factors can be obtained in tunable devices employing BZN films.

At low frequencies (< 100 MHz) electrical characteristics can be obtained using relatively large area metal-insulator-metal (MIM) capacitor structures to estimate relative permittivities, losses, and tunabilities of the films. At microwave frequencies, resistive and inductive parasitics in the capacitors strongly influence the electrical measurements and data interpretation [12,13]. Devices with a small area are advantageous because they have a lower intrinsic capacitance, thus avoid self-resonance, and minimize extrinsic losses. However, small device areas lead to increased Ohmic loss, and the high intrinsic capacitance densities of thin films of tunable dielectrics such as BZN and BST require electrode areas that are smaller than typical on-wafer probe tips, making measurements challenging. In this work, relatively thick (~300 nm) BZN films were used for the microwave characterization to alleviate these problems. Rectangular MIM capacitors with areas between 50 and 900 μm^2 were fabricated that were subsequently interconnected to a larger metal contact or transmission-line that was probe-able.

II. EXPERIMENTAL

200 nm Pt/25 nm Ti bottom electrodes were deposited on sapphire and vycor glass substrates, respectively. Electrodes were patterned by a lift-off process to simplify subsequent processing and to reduce resistive and reactive parasitics. BZN films were deposited by rf magnetron sputtering, as described elsewhere [3,14]. The substrate temperature was maintained at 300 ºC during deposition. BZN films were patterned

using a 1:10 HF – de-ionized H_2O solution. Films were amorphous after deposition and were annealed at 750 ºC in air after patterning to crystallize the films. The leakage currents of 12 × 12 μm capacitors were approximately 7×10^{-7} A/cm^2 at an applied field of 1.2 MV/cm (the leakage was too small to measure at zero applied voltage) and the breakdown fields were greater than 2.4 MV/cm for thin (160 nm) films and about 1.8 MV/cm for thick (320 nm) films. The leakage current are thus much lower and the break down fields higher than state-of-the art BST films [15].

A schematic of the device used for microwave measurements is shown as inset in Fig. 1. A thin (200 nm) SiO_2 layer was used as a dielectric crossover on the bottom electrode edge. The top electrodes (500 nm electron beam evaporated Au) were patterned by a lift-off process, followed by a rapid thermal anneal at 700 ºC for 30 s [3]. A thick (1 μm) Au metal interconnect layer was evaporated to form the low-resistance interconnects and probe pads.

II. RESULTS AND DISCUSSION

Depending on their size, the device capacitances ranged between 0.1 and 4 pF. The maximum tunability was ~ 30% for the microwave devices (Fig. 1). This tunability was less than that of larger area devices on unpatterned bottom electrodes used for low-frequency measurements [3], shown for comparison in Fig. 1. The lower tunability of the films in the microwave devices was due to a lower dielectric strength that did not permit the application of large enough fields required for high tunabilities. The lower breakdown strength may be due to degradation of the air-exposed pre-patterned electrode or due to field concentration at the edges. Modifications of the device are underway.

The complex reflection coefficients (S_{11}) of the devices were measured using a Vector Network Analyzer (Agilent 8510) and a probe station with coplanar waveguide GSG probes (Cascade Microtech APC40). A one-port Short-Open-Load (SOL) calibration was performed using laser-trimmed impedance standards substrates (ISS, Cascade Microtech). Figure 2 shows the measured reflection coefficient of a capacitor on sapphire from 1.5 to 20 GHz plotted in the complex plane with normalized impedance curves superimposed (Smith chart [16]). The plot showed that the data were close to the outmost circle of the Smith chart, indicating that the device showed excellent loss characteristics over the entire frequency range. Since the accuracy of the network analyzer is somewhat limited for reactive loads with higher or lower impedances relative to the normalized impedance Z_0, care must be taken during calibration. Signal averaging and a reduced intermediate frequency (IF) bandwidth on the network analyzer improved the measurement accuracy.

The total device impedance Z_{DUT} of device under test (DUT), including all parasitics, such as those from the large probe pads, was calculated from the measured reflection coefficient:

$$Z_{DUT} = Z_0 \frac{1 + S_{11}}{1 - S_{11}} = \mathrm{Re}(Z_{DUT}) + i\,\mathrm{Im}(Z_{DUT}) \qquad (1)$$

where Z_0 is the characteristic impedance of the transmission cable (50 Ω). The total device quality factor (Q_{DUT}) and capacitance (C_{DUT}) were calculated using $Q_{DUT} = \mathrm{Im}(Z_{DUT})/\mathrm{Re}(Z_{DUT})$ and $C_{DUT} = -\left[2\pi f\,\mathrm{Im}(Z_{DUT})\right]^{-1}$ (Fig. 3(a)). All calculations were carried out using Agilent's Advanced Design System (ADS) software. Furthermore, the parasitics due to the large pads used to connect the BZN capacitors must be estimated and de-embedded to obtain the intrinsic device characteristics. The sharp

upturn in capacitance in Fig. 3 (a) is due to the series inductance in the probe pads, which leads to a self-resonance frequency. By definition, Q_{DUT} goes to zero at resonance. The de-embeeding was done using calibration pads, i.e. open and short structures on the same wafer [12,13,17]. The open structures omitted the DUT and left the pads open. The shorted devices connected the signal and ground plates where the DUT would have been located. The intrinsic capacitor impedance Z_{int} was then given by [12,17]

$$Z_{\text{int}} = \frac{Z_{op}^2 (Z_{DUT} - Z_{sh})}{(Z_{op} - Z_{DUT})(Z_{op} - Z_{sh})}\Big|_{Z_{op} \to \infty} \quad \to (Z_{DUT} - Z_{sh}) \tag{2}$$

where Z_{op} and Z_{sh} are the short and open device impedances. Figure 3 (b) shows the estimated intrinsic capacitor device quality factor, Q_{int}, and capacitance, C_{int}, for two devices with different areas ($Q_{\text{int}} = \text{Im}(Z_{\text{int}})/\text{Re}(Z_{\text{int}})$ and $C_{\text{int}} = -[2\pi f \,\text{Im}(Z_{\text{int}})]^{-1}$).

The device capacitance C_{int} showed very little dispersion, only a slight decrease with frequency following a power-law with a small exponent (~ - 0.002), as would be expected for a nearly constant loss tangent. There was no indication of an onset of a dielectric relaxation, which would exhibit a much stronger frequency dependence [7]. The quality factor Q_{int} was frequency dependent but remained above 200 up for frequencies up to 20 GHz and around 1000 up to several GHz for the smaller device. The large scatter in the high Q-factor data is a limitation of network analyzer measurements as the device reactance moves away from 50 Ohms. The observed device area or periphery dependence of the quality factor Q_{int} is presently not understood but has also been observed for high-Q BST thin film capacitors [17]. The results suggest that the device performance at high frequencies is not limited by intrinsic BZN film losses, because such losses would be area (or periphery)-independent and would be accompanied by a stronger

capacitive dispersion. The decrease in device quality factor with increase in frequency is at least partially due to electrode conductor losses, which in the absence of other effects can easily dominate the device quality factor in small-area capacitors at high frequencies [3,18]. Low-frequency measurements of large-area capacitors showed that the contributions of electrode losses to the device quality factor became significant above 100 MHz [3]. The contributions of top and bottom electrodes may depend on device geometry [17]. It is also possible that an interfacial layer at the metal/dielectric interface that cannot be neglected at microwave frequencies contributes to the device quality factor [19]. Work is underway to reduce the contribution from the bottom electrode to the device Q-factor by using thicker electrodes with a higher conductivity [18,20] and by optimizing the device design.

For bulk BZN, losses ($\tan\delta = Q^{-1}$) of ~ 0.03 (or $Q = 33$) at 1 GHz and ~ 0.12 (or $Q = 8.3$) at 10 GHz have been reported [9]. Thus, despite significant contributions from the electrodes and other unaccounted parasitics to the device Q-factor, the much higher Q-factors of thin film devices showed that the BZN thin films investigated in this study had much lower intrinisic losses than bulk BZN at similar frequencies. Our previous investigations have shown that the dielectric relaxation of BZN thin films is sensitive to film stress [10], but further investigations are clearly needed to fully understand the origins of the differences between BZN thin film and bulk dielectric behavior.

Although difficult to compare due to very different device layouts and electrodes, the device Q-factors of BZN film capacitors are higher than the best reported BST thin film capacitors in the same frequency range [20], which show Q-factors of ~ 100 at 10 GHz. The device Q-factors are also much higher than the best BST devices using similar

device layouts [17]. At 1 GHz, the dielectric tunability is similar to that of BST devices optimized for low losses at microwave frequencies [20,21]. Optimization of the electrodes and device designs will likely further improve the performance of the microwave BZN film capacitors, including tunability and device *Q*-factors, which should make BZN films very attractive for applications in tunable matching networks and voltage-controlled devices in the GHz range.

ACKNOWLEDGEMENTS

This research was supported by the Army Research Office MURI program, grant #DAAD19-01-1-0496 and by NSF (grant # DMR-0307914). We thank Ms. Nadia Pervez for the leakage measurements.

References

1. A. K. Tagantsev, V. O. Sherman, K. F. Astafiev, J. Venkatesh, and N. Setter, J. Electroceram. **11,** 5 (2003).
2. I. Levin, T. G. Amos, J. C. Nino, T. A. Vanderah, C. A. Randall, and M. T. Lanagan, J. Solid State Chem. **168,** 69 (2002).
3. J. W. Lu and S. Stemmer, Appl. Phys. Lett. **83,** 2411 (2003).
4. W. Ren, S. Trolier-McKinstry, C. A. Randall, and T. R. Shrout, J. Appl. Phys. **89,** 767 (2001).
5. Y. P. Hong, S. Ha, H. Y. Lee, Y. C. Lee, K. H. Ko, D. W. Kim, H. B. Hong, and K. S. Hong, Thin Solid Films **419,** 183 (2002).
6. R. L. Thayer, C. A. Randall, and S. Trolier-McKinstry, J. Appl. Phys. **94,** 1941 (2003).
7. J. C. Nino, M. T. Lanagan, and C. A. Randall, J. Appl. Phys. **89,** 4512 (2001).
8. D. P. Cann, C. A. Randall, and T. R. Shrout, Solid State Commun. **100,** 529 (1996).
9. J. C. Nino, M. T. Lanagan, C. A. Randall, and S. Kamba, Appl. Phys. Lett. **81,** 4404 (2002).
10. J. W. Lu, D. O. Klenov, and S. Stemmer, Appl. Phys. Lett. **84,** 957 (2004).
11. Y. C. Chen, H. F. Cheng, G. Wang, X. D. Xiang, C. M. Lei, and I. N. Lin, Jap. J. Appl. Phys. Part 1 **41,** 7214 (2002).
12. K. Ikuta, Y. Umeda, and Y. Ishi, Jpn. J. Appl. Phys. Part 2 **34** (1995).
13. J. D. Baniecki, R. B. Laibowitz, T. M. Shaw, P. R. Duncombe, D. A. Neumayer, D. E. Kotecki, H. Shen, and Q. Y. Ma, Appl. Phys. Lett. **72,** 498 (1998).
14. J. W. Lu, Z. Q. Chen, T. R. Taylor, and S. Stemmer, J. Vac. Sci. Technol. A **21,** 1745 (2003).
15. G. W. Dietz, M. Schumacher, R. Waser, S. K. Streiffer, C. Basceri, and A. I. Kingon, J. Appl. Phys. **82,** 2359 (1997).
16. P. H. Smith, *Electronic applications of the Smith chart*, 2nd ed. (Noble Publishing, Atlanta, 2000).
17. B. Acikel, Ph.D. Thesis, University of California Santa Barbara, 2002.
18. D. C. Dube, J. Baborowski, P. Muralt, and N. Setter, Appl. Phys. Lett. **74,** 3546 (1999).
19. H. Rohdin, N. Moll, A. M. Bratkovsky, and C.-Y. Su, Phys. Rev. B **59,** 13102 (1999).
20. A. Vorobiev, P. Rundqvist, K. Khamchane, and S. Gevorgian, Appl. Phys. Lett. **83,** 3144 (2003).
21. A. K. Tagantsev, J. W. Lu, and S. Stemmer, Appl. Phys. Lett. **86,** 032901 (2005).

Figure captions

Figure 1 (color online)

Bias field dependence of the permittivity of a ~ 150 nm thick BZN film in a planar vycor/Pt/BZN/Pt capacitor structure (capacitor area: 2000 μm^2, open blue symbols) and a microwave capacitor with an area of 360 μm^2 (full black symbols), both measured at 1 MHz. Measurements were performed using an impedance analyzer (Agilent 4294A) and on-wafer GSG probes. The insets show a schematic cross-section of the microwave capacitor (bottom center) and a photograph of the device (upper left corner).

Figure 2 (color online)

Reflection coefficient (S_{11}) of a BZN thin film capacitor on a sapphire substrate plotted on a Smith Chart for a 100 μm^2 capacitor.

Figure 3 (color online)

(a) The total device quality factor (black) and capacitance (blue) for BZN capacitors on sapphire substrates for two devices with different areas. (b) Extracted device quality factor Q_{int} (black) and capacitance C_{int} (blue) for BZN capacitors on sapphire substrates after accounting for pad parasitics (Eqn. 2) for two devices. Open circles represent the device with an area of 100 μm^2 and full symbols the device with an area of 225 μm^2, respectively.

Figure 1

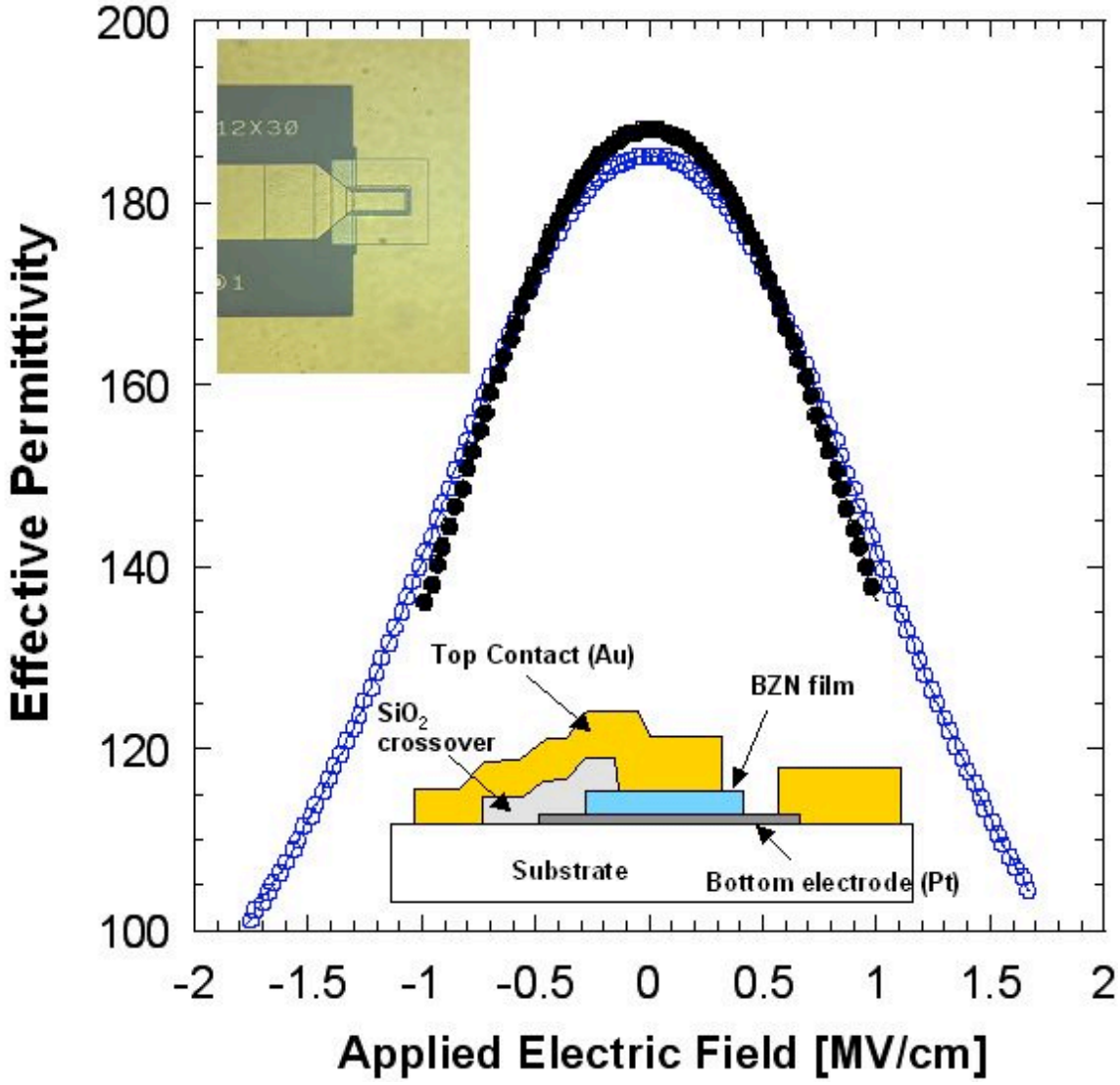

Park *et al.*, Figure 1

Figure 2

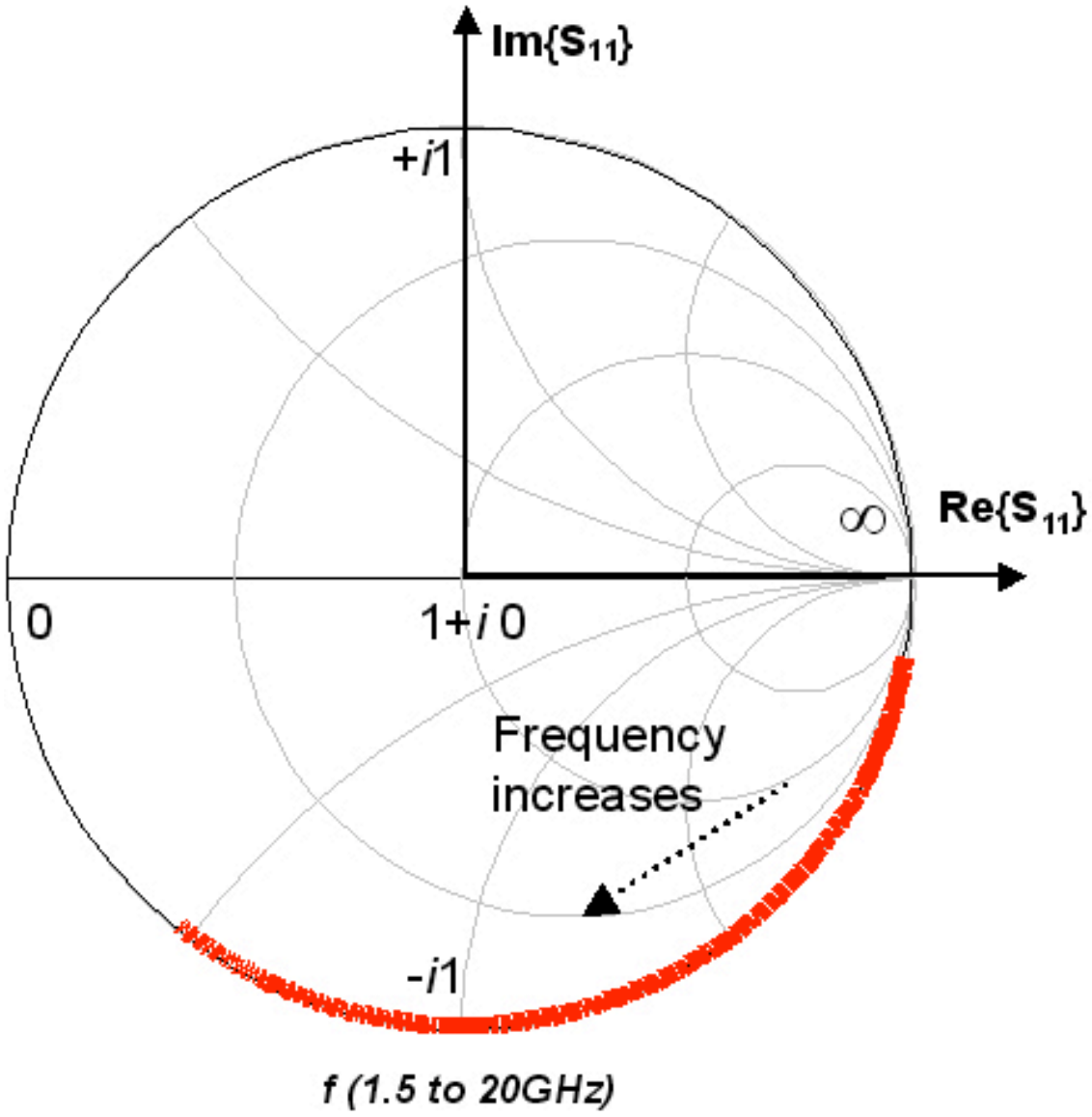

Park *et al.*, Figure 2

Figure 3 (a)

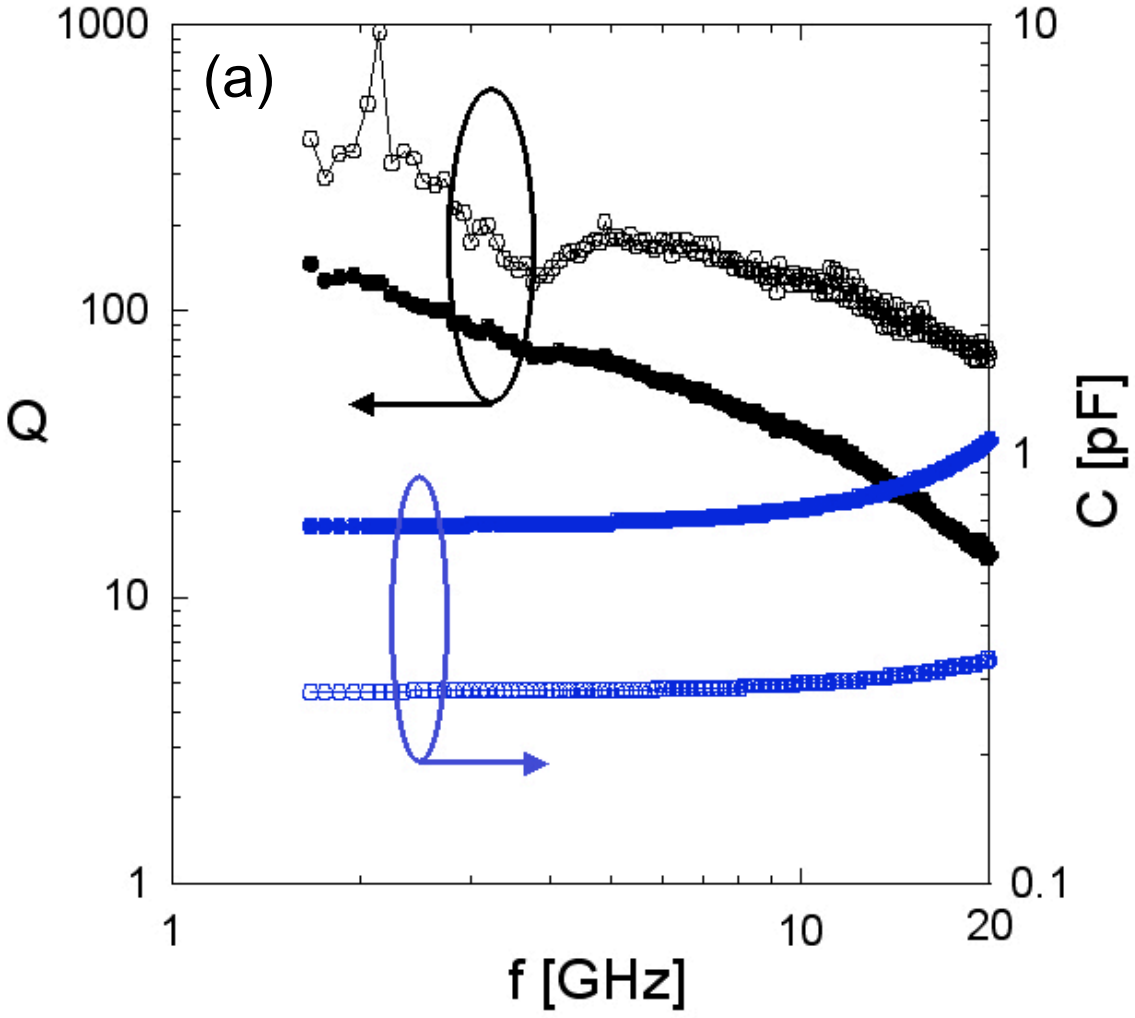

Park *et al.*, Figure 3 (a)

Figure 3 (b)

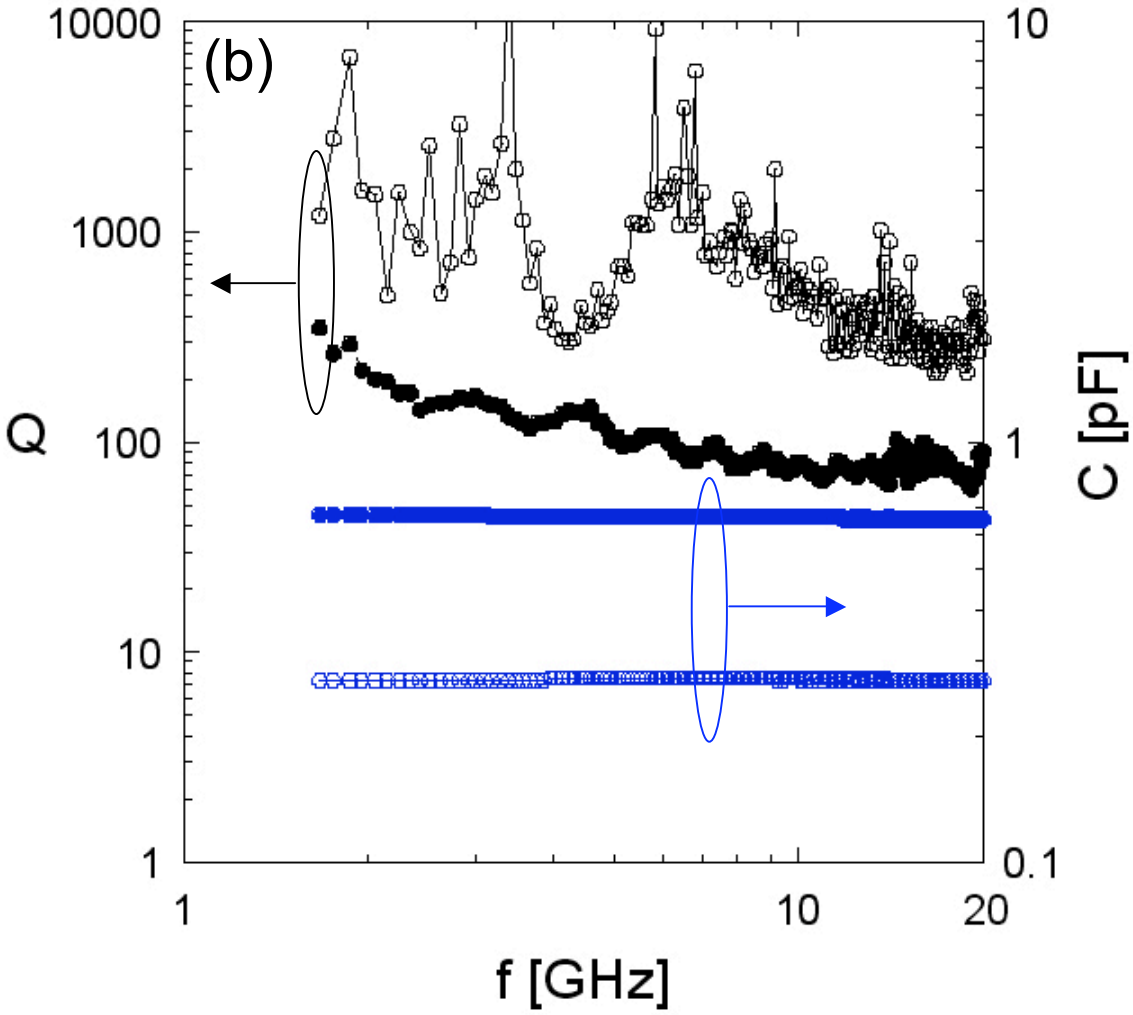

Park *et al.*, Figure 3 (b)